Novel discretization method to calculate g-functions of vertical geothermal boreholes with improved accuracy and efficiency

Yue Yang^a, Xiaodong Yang^a, Chenhui Lin^b, Luo Xu^c, Qi Wang^d, Shuwei Xu^b, Wenchuan Wu^b

^aState Key Laboratory of High-Efficiency and High-Quality Conversion for Electric Power, Hefei University of Technology, Hefei, 230009, China
 ^bState Key Laboratory of Power Systems, Department of Electrical Engineering, Tsinghua University, Beijing, 100084, China
 ^cDepartment of Civil and Environmental Engineering, Princeton University, Princeton, 08544, USA
 ^dThe Hong Kong Polytechnic University, Hong Kong, 999077, China

Abstract

The calculation of g-functions is essential for the design and simulation of geothermal boreholes. However, existing methods, such as the stacked finite line source (SFLS) model, face challenges regarding computational efficiency and accuracy, particularly with fine-grained discretization. This paper introduces a novel discretization method to address these limitations. We reformulate the g-function calculation under the uniform borehole wall temperature boundary condition as the solution to spatio-temporal integral equations. The SFLS model is identified as a special case using stepwise approximation of the heat extraction rate. Our proposed method employs the Gauss-Legendre quadrature to approximate the spatial integrals with a weighted sum of function values at strategically chosen points. This transforms the time-consuming segment-to-segment integral calculations in SFLS model into simpler and analytical point-to-point response factors. Furthermore, we identify that the governing integral equations are of the Fredholm first kind, leading to ill-conditioned linear systems that can cause g-function to diverge at high discretization orders. To address this, a regularization technique is implemented to ensure stable and convergent solutions. Numerical tests demonstrate that the proposed method is significantly more efficient, achieving comparable or improved accuracy at speeds 20 to 200 times faster than the SFLS model with optimized nonuniform discretization schemes.

Keywords:

geothermal energy, borehole heat exchanger, g-function, discretization method, numerical simulation

1. Introduction

Geothermal boreholes are the critical interface for heat exchange in ground source heat pump (GSHP) [1, 2] and borehole thermal energy storage (BTES) systems [3]. These technologies are cornerstones in the global effort to decarbonize building heating and cooling, leveraging the earth's stable subsurface temperature for exceptional energy efficiency. Coupled with BTES, these systems further enable the seasonal shifting of thermal energy, storing excess heat or cold from renewable sources or waste heat for later use. Such integrated solutions not only reduce reliance on fossil fuels but also enhance grid resilience by balancing supply-demand mismatches in renewable-dominated energy systems.

The thermal performance of these systems hinges on the heat exchange capability of the boreholes, which is influenced by their wall temperatures and the ground's thermal properties. Consequently, the efficiency and economic viability of GSHP and BTES systems depend critically on the accurate modeling and simulation of geothermal boreholes, particularly in predicting their long-term thermal response. It is crucial to simulate the temporal evolution of borehole wall temperature accurately with respect to specific heat load patterns to evaluate the long-term thermal performance of geothermal boreholes from a system design and optimization perspective.

g-function, namely the dimensionless thermal response function, is one of the most important tools in the simulation of geothermal boreholes since it is introduced by Eskilson [4]. It has been widely used to design and optimize the performance of GSHP [5, 6] and BTES systems [7]. Once the g-function of a group of boreholes is known, the effective borehole wall temperature T can be written as a convolution in time domain:

$$T(t) = T_g - \frac{1}{2\pi k} \int_0^t Q(t-\tau) \frac{dg}{dt}(\tau) d\tau$$
 (1)

where T_g is the undisturbed ground temperature, k is the thermal conductivity of the ground, Q(t) is the average heat extraction rate per length of borehole, and g(t) is the g-function of borehole field. The g-function is a function of time that describes the temperature response of the borehole wall to a unit heat extraction rate per length applied at time t = 0. The temporal convolution can be computed efficiently with fast fourier transform (FFT) [8, 9] and various load aggregation methods [10, 11].

The computation of g-function is a challenging task due to the complex heat transfer processes involved inside and outside geothermal boreholes. Numeric finite difference models can be used to solve the partial differential equations governing thermal process and obtain the values of g-functions, including the superposition borehole model (SBM) proposed by Eskilson [4], the duct ground storage model (DST) used in TRNSYS [12] and more general finite element methods (FEM) software like COMSOL [13] or OpenGeoSys [14]. However, numerical methods are computationally expensive and time-consuming, especially for large bore fields with many boreholes and long simulation periods, which drives the development of analytical models of g-functions for clear physical interpretation and more efficient calculation.

Among analytical models, finite line source (FLS) is the most widely used approach to analyze the thermal behavior of geothermal boreholes, which ignores the geometric details of boreholes and assumes that each borehole is a line heat source with finite length in a semi-infinite ground. The influence of heat exchange on the temperature of borehole walls can be acquired via spatial and temporal superposition. The study of FLS model can be dated back to the original definition of g-function by Eskilson [4], then rediscovered by various researchers including Zeng [15], Lamarche [16] and broadened to inclined boreholes in [17] and [18].

These early studies on FLS usually assumes that the heat exchange rate is a constant value along the depth of borehole and calculates their influence on the borehole wall temperature at specific points or the average temperature of the whole borehole. This assumption leads to the depth-dependent distribution of borehole wall temperature and is not well aligned with the boundary condition used by Eskilson's original SBM model to compute g-function, which assumes that the borehole wall temperature is uniform along the depth of borehole and the heat exchange rate is a depth-dependent variable. The discrepancy between the boundary conditions results in the overestimation of g-function given by FLS model compared to SBM model, as pointed out by several researchers in [16, 19, 20].

The seminal work of Cimmino [21] fulfills the gap of boundary conditions by dividing the borehole into segments and assuming that the heat exchange rate is constant in each segment but different across segments, which is called stacked finite line source (SFLS) model. They discuss three kinds of boundary conditions (BC) for FLS model of boreholes, where the depth-agnostic constant heat exchange rate is refered as BC-I and the uniform borehole wall temperature (UBWT) is named after BC-III. The SFLS model can approximate the uniform borehole wall temperature boundary condition (BC-III) used in SBM model by constraining the average temperature of each segment to be equal, and the g-function calculated by SFLS model is consistent with SBM model with significantly lower computational time. The methodology of SFLS model under BC-III is validated by FEM models with similar boundary conditions in [22] and generalized from vertical boreholes to inclined boreholes in [23, 24]. Cimmino further extends the SFLS model to calculate g-function under more boundary conditions considering the thermal resistance [25], the connection topology of boreholes [26] and variable mass flow rates [27]. Open source implementation of SFLS model is also available in the pygfunction package [28, 29] with support for various boundary conditions and borehole configurations.

The accuracy and efficiency of SFLS model depends on the number of segments and the length of each segment to discretize the borehole and approximate the depth-varying heat exchange rate. Increasing the

number of segments generally leads to a more accurate representation of the borehole's thermal response, as it allows for a finer resolution of the heat exchange process along the borehole's depth. Researchers have observed that the number of segments per borehole required to achieve acceptable precision of q-function increases as the number of boreholes grow [30]. Nevertheless, the computational time of SFLS model increases quadratically with respect to the total number of segments [30] because the segment-to-segment heat response factor has to be computed for each pair of segments, so the number of segments is usually limited to a small value in practice. Cimmino [21] tests the accuracy of SFLS model up to 256 segments and suggests to use 12 segments per borehole as an approximation. Lamarche [31] proposes a revised SFLS model to assume linear variation of heat extraction rate within each segment and concludes that 8 segments per borehole is sufficient to achieve accuracy of 12 segments per borehole with conventional SFLS. Cook [30] explores the idea of nonuniform discretization of boreholes, where the segments are denser near the beginning and ending of borehole to describe the rapid variation of heat extraction rate, and shows that 8 unequal segments can achieve better accuracy than uniform discretization with the same number of segments. Their sequential research [32] aims to optimize the nonuniform discretization scheme by minimizing the error of q-function tested on a large corpus of 557056 bore field configurations. However, existing work on the discretization scheme of SFLS model is mostly based on empirical experimentation on numerous simulations and lacks formal theoretical foundations. It is still an open problem on the existence of better discretization scheme to reduce both the error and computational time of g-function for geothermal boreholes.

In this paper, we aim to provide new insights on the g-function of boreholes under UBWT boundary condition from the perspective of integral equations and propose a novel discretization scheme to improve the accuracy and efficiency of g-function computation compared with existing SFLS model. The main contributions of our paper can be summarized as answers to the following questions that are crucial for calculating g-functions of boreholes:

1. Why does detailed discretization of boreholes lead to more accurate g-function?

We find out that g-function is essentially the solution to a group of spatio-temporal integral equations describing the thermal process of boreholes under specific boundary conditions, and the segmentation of borehole can be regarded as discrete approximation of the original continuous heat extraction rate with respect to the depth and its spatial integral. The error of approximation naturally decreases as the order of discretization grows because it captures more spatial details of the heat exchange process on the borehole wall. Under this framework, the widely-used SFLS model is a special discretization scheme of the integral equation by assuming the heat exchange rate as a stepwise function that remains constant in each segment.

2. How can we acquire more accurate g-function with limited order of discretization?

We propose a novel discretization scheme that approximates the spatial integral of heat extraction with Gauss-Legendre quadrature rule, which can achieve better accuracy than the SFLS model with the same order of discretization due to the rapid convergence of Gauss-Legendre quadrature. Instead of assuming a constant heat exchange rate within each segment, this approach only requires the value of heat extraction rate at some strategically chosen points at specific depths, so the segment-to-segment coupling factors in SFLS that are time-consuming to calculate as integral are reduced to much simpler point-to-point coupling factors with analytical form. Thus, the computation of g-function can be significantly accelerated due to the faster convergence rate with respect to discretization and more efficient formulation of the discretized equations. It is observed that the proposed method can obtain the g-function with similar or lower error at 20-200 times faster speed compared to SFLS model.

3. Will the value of g-function always converge if the order of discretization is sufficiently large?

It is an intuitive assumption that increasing order of discretization will lead to a converged value of g-function. However, this conjecture is not thoroughly discussed or proved in previous research. In this paper, we discover that the integral equations under UBWT boundary condition belong to the Fredholm integral equation of the first kind. Its discretized linear forms will be ill-conditioned if the order of discretization becomes too large and may fail to provide a meaningful value of g-function. The divergence of g-function is demonstrated by our numerical tests for both SFLS model and the proposed

discretization method. A regularization technique is developed to overcome the ill-conditioning and ensure the stable convergence of g-function under arbitrary discretization. As far as we know, this is the first time that the convergence of g-function is discussed in the context of integral equations and the unintuitive divergence of g-function is explained by the ill-condition of discretized equations.

The paper is structured as follows. In Section 2, we present the methodology used in this study, including the formulation of the integral equations, the SFLS model as an approximation and the proposed discretization scheme. Section 3 provides the numerical results and comparisons between the proposed method and existing models. Finally, we conclude the paper in Section 4.

2. Methodology

2.1. Heat extraction rate and wall temperature of borehole

Consider a three-dimensional infinite isotropic medium with uniform thermal properties including thermal conductivity k and thermal diffusivity α . An instantaneous point heat source extracts energy Q at the origin (r=0), then the temperature change induced by this heat source at arbitrary point is dependent on the elapsed time t and the distance to the heat source d, given by the product of Q and Green function K(d,t) [33].

$$\Delta T(d,t) = -QK(d,t) \tag{2}$$

$$K(d,t) = \frac{1}{\rho c (4\pi\alpha t)^{\frac{3}{2}}} \exp\left(-\frac{d^2}{4\alpha t}\right)$$
(3)

The integral of K(d,t) over time from t_1 to t_2 is provided for reference where erfc is the complementary error function.

$$J(d, t_1, t_2) = \int_{t_1}^{t_2} K(d, \tau) \ d\tau = \frac{1}{4\pi k d} \left(\operatorname{erfc} \left(\frac{d}{2\sqrt{\alpha t_2}} \right) - \operatorname{erfc} \left(\frac{d}{2\sqrt{\alpha t_1}} \right) \right)$$
(4)

$$J(d,0,t_2) = \int_{t_1}^{t_2} K(d,\tau) d\tau = \frac{1}{4\pi k d} \operatorname{erfc}\left(\frac{d}{2\sqrt{\alpha t_2}}\right)$$
 (5)

$$\operatorname{erfc}(x) = \frac{2}{\sqrt{\pi}} \int_{x}^{\infty} e^{-t^{2}} dt \tag{6}$$

For a bore field composed of multiple vertical boreholes, we assume there are N_b vertical boreholes located at positions (x_i, y_i) for $i = 1, 2, \ldots, N_b$ and with buried depth D_i and length H_i . The total temperature change at a point (x, y, z) due to all boreholes can be obtained by summing the contributions from each borehole. Each borehole is regarded as a line composed of many point heat sources, and the heat extraction and wall temperature of each borehole varies along the depth in ground and time, so we assume that the heat extraction rate per length and wall temperature is a bivariate function with respect to both depth and time expressed as Q(z,t) and T(z,t), respectively. As shown in Figure 1, we introduce mirror boreholes with opposite heat extraction rate above the ground to maintain constant temperature at the ground surface as T_g , namely the undisturbed ground temperature.

The temperature at arbitrary point (X, Y, Z) and a specific time t is given by the temporal and spatial superposition:

$$T(X,Y,Z,t) = T_g - \sum_{i=1}^{N_b} \int_{D_i}^{D_i + H_i} \int_0^t Q_i(z,\tau) K(r(X-x_i,Y-y_i,Z-z),t-\tau) \ d\tau dz$$

$$+ \sum_{i=1}^{N_b} \int_{D_i}^{D_i + H_i} \int_0^t Q_i(z,\tau) K(r(X-x_i,Y-y_i,Z+z),t-\tau) \ d\tau dz$$
(7)

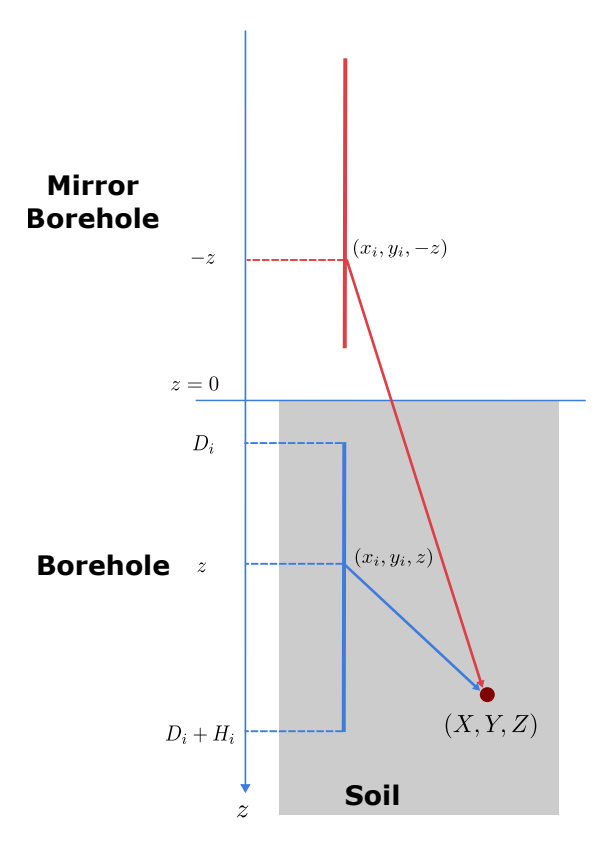


Figure 1: Spatial superposition of boreholes and their mirrors

$$r(x, y, z) = \sqrt{\max(x^2 + y^2, r_b^2) + z^2}$$
(8)

If the heat extraction rate is discretized into T_{max} slots at points $t_0 = 0, t_1, t_2, \dots, t_{T_{max}}$, we notice that:

$$\int_{0}^{t_{k}} Q_{i}(z,\tau)K(d,t-\tau) d\tau = \sum_{p=1}^{k} Q_{i}(z,t_{p}) \int_{t_{p-1}}^{t_{p}} K(d,t-\tau) d\tau
= \sum_{p=1}^{k} Q_{i}(z,t_{p}) \int_{t-t_{p}}^{t-t_{p-1}} K(d,\tau) d\tau
= \sum_{p=1}^{k} Q_{i}(z,t_{p})J(d,t-t_{p},t-t_{p-1})$$
(9)

So, we have:

$$T(X,Y,Z,t_k) = T_g - \sum_{p=1}^k \sum_{i=1}^{N_b} \int_{D_i}^{D_i+H_i} Q_i(z,t_p) J(r(X-x_i,Y-y_i,Z-z),t_k-t_p,t_k-t_{p-1}) dz$$

$$+ \sum_{p=1}^k \sum_{i=1}^{N_b} \int_{D_i}^{D_i+H_i} Q_i(z,t_p) J(r(X-x_i,Y-y_i,Z+z),t_k-t_p,t_k-t_{p-1}) dz$$

$$(10)$$

The
$$\sum_{p=1}^{k}$$
 summation means the temporal superposition and $\sum_{i=1}^{N_b} \int_{D_i}^{D_i + H_i}$ denotes the spatial superposition

from all boreholes and their mirrors. The contribution of each borehole is written as an integral along its depth to accumulate the influence of varying heat extraction rate. r is the distance from target point (X,Y,Z) to the source point (x_i,y_i,z) and its mirror $(x_i,y_i,-z)$. r_b is the radius of each borehole to avoid singularity when the target point is on the wall of borehole $(x=x_i \text{ and } y=y_i)$. If the coordinates (X,Y,Z) is set at the borehole wall (x_i,y_i,Z) , this formula gives the borehole wall temperature.

We separate the expression of temperature into two parts to discriminate the contributions from previous time-steps and current time-step:

$$T(X,Y,Z,t_{k}) = T_{0}(X,Y,Z,t_{k})$$

$$-\sum_{i=1}^{N_{b}} \int_{D_{i}}^{D_{i}+H_{i}} Q_{i}(z,t_{k})J(r(X-x_{i},Y-y_{i},Z-z),0,t_{k}-t_{k-1}) dz$$

$$+\sum_{i=1}^{N_{b}} \int_{D_{i}}^{D_{i}+H_{i}} Q_{i}(z,t_{k})J(r(X-x_{i},Y-y_{i},Z+z),0,t_{k}-t_{k-1}) dz$$
(11)

$$T_{0}(X, Y, Z, t_{k}) = T_{g}$$

$$-\sum_{p=1}^{k-1} \sum_{i=1}^{N_{b}} \int_{D_{i}}^{D_{i}+H_{i}} Q_{i}(z, t_{p}) J(r(X - x_{i}, Y - y_{i}, Z - z), t_{k} - t_{p}, t_{k} - t_{p-1}) dz$$

$$+\sum_{p=1}^{k-1} \sum_{i=1}^{N_{b}} \int_{D_{i}}^{D_{i}+H_{i}} Q_{i}(z, t_{p}) J(r(X - x_{i}, Y - y_{i}, Z + z), t_{k} - t_{p}, t_{k} - t_{p-1}) dz$$

$$(12)$$

In the context of g-function (thermal response function), the average heat extraction rate per length is constant:

$$Q(t_k) = \frac{\sum_{i=1}^{N_b} \int_{D_i}^{D_i + H_i} Q_i(z, t_k) dz}{\sum_{i=1}^{N_b} H_i} = 1$$
(13)

As discussed in [21], we need extra boundary conditions to solve the value of g-function, and the uniform borehole wall temperature (UBWT) boundary condition is chosen in this paper, which assumes that all the borehole walls have the same time-varying temperatures:

$$T(x_i, y_i, z, t_k) = T(t_k)(i = 1, 2, \dots, N_b, D_i \le z \le D_i + H_i)$$
 (14)

11, 12, 13 and 14 are the governing integral equations of bore field that describes the spatio-temporal evolution of heat extraction rate and borehole wall temperature under UBWT boundary condition. Our goal is to obtain the spatial distribution and temporal evolution of the heat exchange rate $Q_i(z, t_k)$ and uniform temperature of the borehole wall $T(t_k)$.

If we recall the definition of g-function, it is obvious that g-function at time t_k is directly related to the uniform borehole wall temperature if equation 13 holds.

$$T(t) = T_g - \frac{1}{2\pi k} \int_0^t Q(t - \tau) \frac{dg}{dt}(\tau) \ d\tau = T_g - \frac{1}{2\pi k} g(t)$$
 (15)

In the next section, we will discuss how to solve these integral equations to acquire the g-function of bore field under UBWT boundary condition.

Note: The equations can be solved from t_1 to $t_{T_{max}}$ recursively. If we know the distribution of heat extraction rate per length of each bore hole $Q_i(z,t)$ at all time-points in front of t_k (including t_k), we can compute $T_0(X,Y,Z,t_{k+1})$ according to 12. Thus, the key is to solve equation 11 for each time-step.

2.2. Stacked finite line source model as approximate solution to integral equations

We notice that integral equations 11, 12 and 13 all contain the spatial integral of the heat extraction rate $Q_i(z, t_k)$ as an unknown function with respect to the depth z. It is difficult to obtain the analytical form of $Q_i(z, t_k)$ as a continuous function, so we need to find an good approximation.

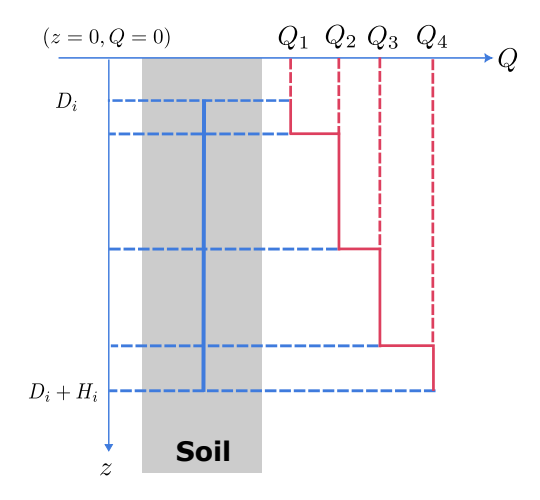


Figure 2: Stacked finite line source model

Stacked finite line source (SFLS) model divides each borehole into segments and approximates $Q_i(z, t_k)$ as a stepwise function that remains constant in each segment. If each borehole is divided into N_s segments, the integral of heat extraction can be decomposed into summation of N_s discrete terms:

$$T(X,Y,Z,t_{k}) = T_{0}(X,Y,Z,t_{k})$$

$$-\sum_{i=1}^{N_{b}} \sum_{j=1}^{N_{s}} Q_{i,j}(t_{k}) \int_{LB_{i,j}}^{UB_{i,j}} J(r(X-x_{i},Y-y_{i},Z-z),0,t_{k}-t_{k-1}) dz$$

$$+\sum_{i=1}^{N_{b}} \sum_{j=1}^{N_{s}} Q_{i,j}(t_{k}) \int_{LB_{i,j}}^{UB_{i,j}} J(r(X-x_{i},Y-y_{i},Z+z),0,t_{k}-t_{k-1}) dz$$

$$(16)$$

$$T_{0}(X, Y, Z, t_{k}) = T_{g}$$

$$- \sum_{p=1}^{k-1} \sum_{i=1}^{N_{b}} \sum_{j=1}^{N_{s}} Q_{i,j}(t_{p}) \int_{LB_{i,j}}^{UB_{i,j}} J(r(X - x_{i}, Y - y_{i}, Z - z), t_{k} - t_{p}, t_{k} - t_{p-1}) dz$$

$$+ \sum_{p=1}^{k-1} \sum_{i=1}^{N_{b}} \sum_{j=1}^{N_{s}} Q_{i,j}(t_{p}) \int_{LB_{i,j}}^{UB_{i,j}} J(r(X - x_{i}, Y - y_{i}, Z + z), t_{k} - t_{p}, t_{k} - t_{p-1}) dz$$

$$(17)$$

where $LB_{i,j}$ and $UB_{i,j}$ are the lower and upper bounds of the j-th segment on the i-th borehole, and $Q_{i,j}(t_k)$ is the average heat extraction rate per length of the j-th segment on the i-th borehole at time t_k .

The UBWT boundary condition 14 is approximated by constraining the average temperature of each segment to be equal. For the n-th segment on the m-th borehole, its average temperature is the same with

the uniform wall temperature $T(t_k)$:

$$T(t_k) = \frac{\int_{LB_{m,n}}^{UB_{m,n}} T(x_m, y_m, z, t_k) dz}{UB_{m,n} - LB_{m,n}}$$
(18)

$$(UB_{m,n} - LB_{m,n})T(t_k) = (UB_{m,n} - LB_{m,n})T_g$$

$$-\sum_{p=1}^{k-1}\sum_{i=1}^{N_b}\sum_{j=1}^{N_s}Q_{i,j}(t_p)\int_{LB_{m,n}}^{UB_{m,n}}\int_{LB_{i,j}}^{UB_{m,n}}J(r(x_m - x_i, y_m - y_i, z_2 - z_1), t_k - t_p, t_k - t_{p-1}) dz_1 dz_2$$

$$+\sum_{p=1}^{k-1}\sum_{i=1}^{N_b}\sum_{j=1}^{N_s}Q_{i,j}(t_p)\int_{LB_{m,n}}^{UB_{m,n}}\int_{LB_{i,j}}^{UB_{i,j}}J(r(x_m - x_i, y_m - y_i, z_2 + z_1), t_k - t_p, t_k - t_{p-1}) dz_1 dz_2$$

$$-\sum_{i=1}^{N_b}\sum_{j=1}^{N_s}Q_{i,j}(t_k)\int_{LB_{m,n}}^{UB_{m,n}}\int_{LB_{i,j}}^{UB_{i,j}}J(r(x_m - x_i, y_m - y_i, z_2 - z_1), 0, t_k - t_{k-1}) dz_1 dz_2$$

$$+\sum_{i=1}^{N_b}\sum_{j=1}^{N_s}Q_{i,j}(t_k)\int_{LB_{m,n}}^{UB_{m,n}}\int_{LB_{i,j}}^{UB_{i,j}}J(r(x_m - x_i, y_m - y_i, z_2 + z_1), 0, t_k - t_{k-1}) dz_1 dz_2$$

The double integral appearing in 19 is called segment-to-segment response factor that reflects how the heat extraction of the j-th segment on the i-th borehole influences the wall temperature of the n-th segment on the m-th borehole. These factors are denoted as:

$$R_{(i,j)\to(m,n)}^+(t_1,t_2) = \int_{LB_{m,n}}^{UB_{m,n}} \int_{LB_{i,j}}^{UB_{i,j}} J(r(x_m - x_i, y_m - y_i, z_2 - z_1), t_1, t_2) \ dz_1 \ dz_2$$
 (20)

$$R_{(i,j)\to(m,n)}^{-}(t_1,t_2) = \int_{LB_{m,n}}^{UB_{m,n}} \int_{LB_{i,j}}^{UB_{i,j}} J(r(x_m - x_i, y_m - y_i, z_2 + z_1), t_1, t_2) \ dz_1 \ dz_2$$
 (21)

According to [34], the segment-to-segment response factor can be expressed as a single integral as follows:

$$\int_{A}^{B} \int_{C}^{D} J(\sqrt{r^{2} + (z_{2} - z_{1})^{2}}, t_{1}, t_{2}) dz_{1} dz_{2}$$

$$= \int_{t_{1}}^{t_{2}} \int_{A}^{B} \int_{C}^{D} \frac{1}{\rho c(4\pi\alpha\tau)^{\frac{3}{2}}} \exp\left(-\frac{r^{2} + (z_{2} - z_{1})^{2}}{4\alpha\tau}\right) dz_{1} dz_{2} d\tau$$

$$= \frac{1}{4\pi k} \int_{1/\sqrt{4\alpha t_{1}}}^{1/\sqrt{4\alpha t_{1}}} \frac{1}{s^{2}} \exp(-r^{2}s^{2}) [ierf((B - C)s)$$

$$- ierf((A - C)s) + ierf((A - D)s) - ierf((B - D)s)] ds$$
(22)

$$\operatorname{erf}(x) = \frac{2}{\sqrt{\pi}} \int_0^x e^{-t^2} dt$$
 (23)

$$ierf(x) = \int_0^x erf(t) dt = xerf(x) - \frac{1}{\sqrt{\pi}} (1 - e^{-x^2})$$
 (24)

Then we can rewrite equation 19 as:

$$(UB_{m,n} - LB_{m,n})T(t_k) = (UB_{m,n} - LB_{m,n})T_g$$

$$-\sum_{p=1}^{k-1}\sum_{i=1}^{N_b}\sum_{j=1}^{N_s}Q_{i,j}(t_p)(R_{(i,j)\to(m,n)}^+(t_k - t_p, t_k - t_{p-1}) - R_{(i,j)\to(m,n)}^-(t_k - t_p, t_k - t_{p-1}))$$

$$-\sum_{i=1}^{N_b}\sum_{j=1}^{N_s}Q_{i,j}(t_k)(R_{(i,j)\to(m,n)}^+(0, t_k - t_{k-1}) - R_{(i,j)\to(m,n)}^-(0, t_k - t_{k-1}))$$
(25)

The average heat extraction rate equation is written as:

$$\frac{\sum_{i=1}^{N_b} \sum_{j=1}^{N_s} (UB_{i,j} - LB_{i,j}) Q_{i,j}(t_k)}{\sum_{i=1}^{N_b} H_i} = 1$$
(26)

Combining N_bN_s equations 25 and the single equation 26 as a linear system, we can solve N_bN_s+1 unknown variables: the average heat extraction rate of each segment $Q_{i,j}(t_k)(1 \le i \le N_b, 1 \le j \le N_s)$ and the uniform borehole wall temperature $T(t_k)$:

$$\begin{bmatrix} \mathbf{A}(0, t_k - t_{k-1}) & \mathbf{1} \\ \mathbf{c}^T & 0 \end{bmatrix} \begin{bmatrix} \mathbf{Q}(t_k) \\ T(t_k) \end{bmatrix} = \begin{bmatrix} \mathbf{1}T_g - \sum_{p=1}^{k-1} \mathbf{A}(t_k - t_p, t_k - t_{p-1}) \mathbf{Q}(t_p) \\ 1 \end{bmatrix}$$
(27)

Therefore, we have derived the core equations of SFLS model under UBWT boundary condition from integral equations that have the same form with [21]. As a discrete approximation of the integral equations, the SFLS model has the following inherent limitations:

- 1. The stepwise approximation of heat extraction rate is discontinuous and not accurate enough to fit the actual continuous spatial distribution of heat flux on borehole wall.
- 2. The numerical simulation has proved that the heat extraction rate experiences rapid change near the heads and tails of borehole and remains flat at the middle of borehole [21, 30], so nonuniform segmentation is required to arrange more segments on both terminals of boreholes to capture the rapid change and reduce the error of approximation. However, there is no theoretical guidance on how to select the appropriate discretization scheme.
- 3. Calculating the segment-to-segment response factors for all pairs of segments as an integral is time consuming and occupies most of the time in computation of g-functions.

2.3. Novel discretization method based on numeric quadrature rule

In this paper, we adopt the Nyström method [35] to solve the integral equation, which is a numerical method to approximate the integral operator with a quadrature rule. For example, the following one-dimensional integral can be approximated by a weighted sum of function values at some specific points:

$$\int_{a}^{b} f(x) dx \approx \sum_{i=1}^{n} w_{i} f(x_{i})$$
(28)

where x_i are the quadrature points and w_i are the corresponding weights. The accuracy of the approximation depends on the number of quadrature points and the selection of quadrature rule.

For the integral equations of boreholes, the spatial integral in 11, 12 and 13 are replaced with a weighted sum with respect to the heat extraction rate per length at some specific depths.

$$T(X,Y,Z,t_{k}) = T_{0}(X,Y,Z,t_{k})$$

$$-\sum_{i=1}^{N_{b}} \sum_{j=1}^{N_{quad}^{heat}} w_{ij}^{heat} Q_{i}(z_{ij}^{heat},t_{k}) J(r(X-x_{i},Y-y_{i},Z-z_{ij}^{heat}),0,t_{k}-t_{k-1})$$

$$+\sum_{i=1}^{N_{b}} \sum_{j=1}^{N_{quad}^{heat}} w_{ij}^{heat} Q_{i}(z_{ij}^{heat},t_{k}) J(r(X-x_{i},Y-y_{i},Z+z_{ij}^{heat}),0,t_{k}-t_{k-1})$$
(29)

$$T_{0}(X, Y, Z, t_{k}) = T_{g}$$

$$-\sum_{p=1}^{k-1} \sum_{i=1}^{N_{b}} \sum_{j=1}^{N_{gaad}} w_{ij}^{heat} Q_{i}(z_{ij}^{heat}, t_{p}) J(r(X - x_{i}, Y - y_{i}, Z - z_{ij}^{heat}), t_{k} - t_{p}, t_{k} - t_{p-1})$$

$$+\sum_{p=1}^{k-1} \sum_{i=1}^{N_{b}} \sum_{j=1}^{N_{gaad}} w_{ij}^{heat} Q_{i}(z_{ij}^{heat}, t_{p}) J(r(X - x_{i}, Y - y_{i}, Z + z_{ij}^{heat}), t_{k} - t_{p}, t_{k} - t_{p-1})$$

$$(30)$$

$$\frac{\sum_{i=1}^{N_b} \sum_{j=1}^{N_{quad}^{heat}} w_{ij}^{heat} Q_i(z_{ij}^{heat}, t_k)}{\sum_{i=1}^{N_b} H_i} = 1$$
(31)

The weight w_{ij}^{heat} and points z_{ij}^{heat} can be determined by arbitrary quadrature rule and we choose Gauss-Legendre rule in this paper. The number of quadrature points N_{quad}^{heat} is a parameter that can be adjusted to control the accuracy of the approximation.

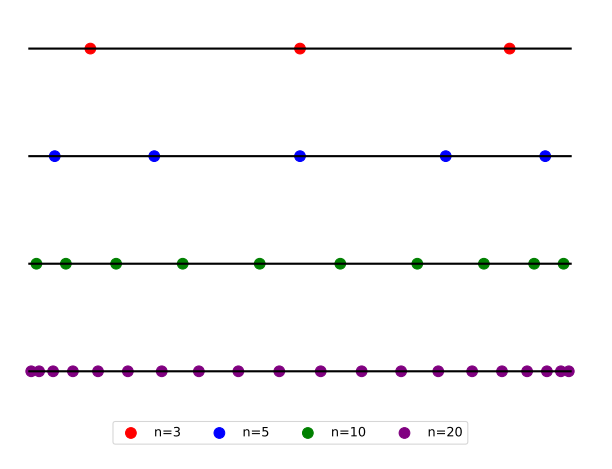


Figure 3: Quadrature points of Gauss-Legendre rule with different order in an interval

As shown in Figure 3, the quadrature points are distributed in the interval nonuniformly with corresponding weights. As the order of quadrature rule increases, the quadrature points are more dense to reduce the error of integral. The locations and weights of quadrature points are pre-calculated and stored in advance.

Similar with the SFLS model, the UBWT boundary condition 14 is approximated by constraining the average temperature of each segment of borehole to be equal. In order to solve $N_b N_{quad}^{heat}$ variables

 $Q(z_{ij}^{heat}, t_k) (1 \le i \le N_b, 1 \le j \le N_{quad}^{heat})$, we separate each borehole into N_{quad}^{heat} segments by the heads and tails of borehole and the midpoints of quadrature points. This segmentation scheme ensures that there is one quadrature point in each segment.

$$LB_{i,j} = \begin{cases} D_i & j = 1\\ \frac{1}{2}(z_{(i-1)j} + z_{ij}), & 1 < j \le N_{quad}^{heat} \end{cases}$$
 (32)

$$UB_{i,j} = \begin{cases} \frac{1}{2} (z_{ij} + z_{(i+1)j}), & 1 \le j < N_{quad}^{heat} \\ D_i + H_i & j = N_{quad}^{heat} \end{cases}$$
(33)

After the segmentation is determined, the integral in 18 is also approximated by a weighted sum of temperatures at quadrature points in each segment according to the same Gauss-Legendre quadrature rule:

$$T(t_k) = \frac{\int_{LB_{m,n}}^{UB_{m,n}} T(x_m, y_m, z, t_k) dz}{UB_{m,n} - LB_{m,n}}$$

$$= \frac{1}{UB_{m,n} - LB_{m,n}} \sum_{l=1}^{N_{quad}^{temp}} w_{mnl}^{temp} T(x_m, y_m, z_{mnl}^{temp}, t_k)$$
(34)

where z_{mnl}^{temp} are the quadrature points in the *n*-th segment on the *m*-th borehole and w_{mnl}^{temp} are the corresponding weights. N_{quad}^{temp} is the number of quadrature points to approximate the integral of temperature in

Substituting the expression of temperature 29 and 30 into 34, we have:

$$(UB_{m,n} - LB_{m,n})T(t_{k}) = (UB_{m,n} - LB_{m,n})T_{g}$$

$$-\sum_{p=1}^{k-1}\sum_{i=1}^{N_{b}}\sum_{j=1}^{N_{b}}w_{ij}^{heat}Q_{i}(z_{ij}^{heat}, t_{p})\sum_{l=1}^{N_{t}^{emp}}w_{mnl}^{temp}J(r(x_{m} - x_{i}, y_{m} - y_{i}, z_{mnl}^{temp} - z_{ij}^{heat}), t_{k} - t_{p}, t_{k} - t_{p-1})$$

$$+\sum_{p=1}^{k-1}\sum_{i=1}^{N_{b}}\sum_{j=1}^{N_{t}^{heat}}w_{ij}^{heat}Q_{i}(z_{ij}^{heat}, t_{p})\sum_{l=1}^{N_{t}^{emp}}w_{mnl}^{temp}J(r(x_{m} - x_{i}, y_{m} - y_{i}, z_{mnl}^{temp} + z_{ij}^{heat}), t_{k} - t_{p}, t_{k} - t_{p-1})$$

$$-\sum_{i=1}^{N_{b}}\sum_{j=1}^{N_{t}^{heat}}w_{ij}^{heat}Q_{i}(z_{ij}^{heat}, t_{k})\sum_{l=1}^{N_{t}^{emp}}w_{mnl}^{temp}J(r(x_{m} - x_{i}, y_{m} - y_{i}, z_{mnl}^{temp} - z_{ij}^{heat}), 0, t_{k} - t_{k-1})$$

$$+\sum_{i=1}^{N_{b}}\sum_{j=1}^{N_{t}^{heat}}w_{ij}^{heat}Q_{i}(z_{ij}^{heat}, t_{k})\sum_{l=1}^{N_{t}^{temp}}w_{mnl}^{temp}J(r(x_{m} - x_{i}, y_{m} - y_{i}, z_{mnl}^{temp} + z_{ij}^{heat}), 0, t_{k} - t_{k-1})$$

$$(35)$$

Combining $N_b N_{quad}^{heat}$ equations 35 and the single equation 31, we can obtain a linear system with the similar structure with 27 to solve $N_b N_{quad}^{heat} + 1$ unknown variables: heat extraction rate of each quadrature point $Q_i(z_{ij}^{heat}, t_k) (1 \le i \le N_b, 1 \le j \le N_{quad}^{heat})$ and the uniform borehole wall temperature $T(t_k)$: Compared with the SFLS model, the proposed formulation has the following advantages:

1. We do not assume the stepwise structure of heat extraction rate $Q_i(z,t_k)$ and only uses limited quadrature points to approximate the integral with numerical quadrature rule, which ensures higher accuracy with the same number of discretization points.

- 2. The discretization scheme to approximate the heat extraction rate and borehole wall temperature are automatically generated by Gauss-Legendre quadrature rule after the number of quadrature points N_{quad}^{heat} and N_{quad}^{temp} are determined, so it is universal for all configurations of bore field and has theoretical guarantee on the accuracy of approximation.
- 3. We only need to compute a series of point-to-point response factors in the form of $J(d, t_1, t_2)$ to formulate the discretized equations. It is analytical and much easier to compute than the segment-to-segment response factor as integral in 22.

2.4. Ill-conditioned discretized equations and regularization

The original integral equations including 11, 12, 13 and 14 can be reduced to the Fredholm integral equation of the first kind:

$$\int_{a}^{b} K(x,y)f(y) \ dy = g(x) \tag{36}$$

where K(x,y) is the kernel function, f(y) is the unknown function to be solved, and g(x) is the known boundary condition. In our case, the kernel function K(x,y) is the response factor $J(d,t_1,t_2)$, the unknown function f(y) is the heat extraction rate $Q_i(z,t_k)$ and the known function g(x) is the uniform borehole wall temperature $T(t_k)$.

The Fredholm integral equation of the first kind is a well-known ill-posed problem [36] where the solution is not unique and sensitive to the perturbation of data. Thus, the discretization of the integral equation in form of linear system 27 is ill-conditioned, and we have observed that its condition number increases quickly with the order of discretization. The ill-conditioned discretized equations lead to numerical instability and incorrect values of q-function, which is confirmed and discussed in the numerical tests.

We use the regularization method proposed in [37] to transform the ill-posed Fredholm integral equation of the first kind into the well-defined second kind with an extra term:

$$\int_{a}^{b} K(x,y)f(y) \ dy = g(x) - \lambda f(x) \tag{37}$$

where λ is a regularization parameter. When λ is small, the solution of 37 is close to the solution of 36. The regularized form of 11 is:

$$T_{reg}(X, Y, Z, t_k) = T(X, Y, Z, t_k) - \lambda Q(X, Y, Z, t_k)$$

$$(38)$$

Then the integral equation 18 in SFLS model is turned into two parts:

$$T(t_k) = \frac{\int_{LB_{m,n}}^{UB_{m,n}} T_{reg}(x_m, y_m, z, t_k) dz}{UB_{m,n} - LB_{m,n}}$$

$$= \frac{\int_{LB_{m,n}}^{UB_{m,n}} T(x_m, y_m, z, t_k) dz}{UB_{m,n} - LB_{m,n}} - \lambda Q_{m,n}(t_k)$$
(39)

It is similar with the proposed discretization method:

$$T(t_k) = \frac{\int_{LB_{m,n}}^{UB_{m,n}} T_{reg}(x_m, y_m, z, t_k) dz}{UB_{m,n} - LB_{m,n}}$$

$$= \frac{\int_{LB_{m,n}}^{UB_{m,n}} T(x_m, y_m, z, t_k) dz}{UB_{m,n} - LB_{m,n}} - \lambda Q_m(z_{mn}^{heat}, t_k)$$
(40)

Table 1: Parameter of geothermal boreholes

Parameter	Value
Buried depth $D(m)$	4.0
Borehole length $H(m)$	120.0
Radius of borehole $r_b(m)$	0.1
Space between borehole(m)	5.0
Thermal diffusivity of soil $\alpha(m^2/s)$	1×10^{-6}

The linear system 27 is modified to the following form where the parameter λ improves the ill-conditioned discretized equations by adding a small diagonal regularization to the coefficient matrix:

$$\begin{bmatrix} \mathbf{A}(0, t_k - t_{k-1}) + \lambda \mathbf{I} & \mathbf{1} \\ \mathbf{c}^T & 0 \end{bmatrix} \begin{bmatrix} \mathbf{Q}(t_k) \\ T(t_k) \end{bmatrix} = \begin{bmatrix} \mathbf{1}T_g - \sum_{p=1}^{k-1} \mathbf{A}(t_k - t_p, t_k - t_{p-1})\mathbf{Q}(t_p) \\ 1 \end{bmatrix}$$
(41)

3. Results

In this section, we will compare the proposed discretized formulation of g-function with the SFLS model in terms of the accuracy, convergence rate and computational efficiency.

Because the accuracy of SFLS model depends on the segementation scheme to discretize the borehole, we choose three different segmentation schemes used in [32] as the targets for comparison. The first one is the uniform segmentation scheme, which divides each borehole into N_s segments with equal length. The second and third one are nonuniform segmentation schemes, which chooses the length of the smallest segments h_1 at both ends of the borehole and arranges the length of segments from the ends to middle of borehole as a geometric series with the common ratio γ . The second scheme chooses $\delta_1 = \frac{h_1}{H} = 0.02 \times \frac{8}{N_s}$ as a baseline and the third scheme chooses $\delta_1 = \frac{h_1}{H} = 0.005525 \times \frac{8}{N_s}$ as the optimal nonuniform discretization trained on dataset including 557056 bore field configurations. The three segmentation schemes are called as "uniform", "nonuniform-base" and "nonuniform-opt" in the rest of paper respectively.

The proposed formulation is implemented in pure Python with NumPy and SciPy libraries. The open source pygfunction module is used as the reference implementation of SFLS model with minimal modifications to add regularization and obtain the condition number of linear system. All numerical tests are performed on a laptop with Intel Core i7-1360P CPU and 32GB RAM.

3.1. The convergence of g-function in a 2-borehole test case

We choose a bore field of two boreholes as a small test case to evaluate the g-functions at ten time points from 2 years to 20 years with a time step of 2 years. The parameters are specified in Table 1.

3.1.1. Divergent g-functions without regularization

In the first round of test, g-function is calculated by solving the original linear system 27 without regularization. The order of discretization is selected as follows:

- ullet The proposed discretization scheme with $N_{quad}^{heat} = [64, 128, 256, 512, 1024]$ and fixed $N_{quad}^{temp} = 40$.
- The SFLS model with $N_s = [64, 128, 256, 512, 1024]$.

The results are shown in Tables 2 to 5 including the condition number of the linear system and the values of g-function at ten time points. We can observe that the value of g-function generally decreases and tends to converge to a stable value as the order of discretization increases from 64 to 1024. The exceptions happen when the order of discretization equals to 1024 for the proposed discretization scheme and the optimal nonuniform discretization scheme, where the value of g-function gradually deviates from

Table 2: g-function of 2 boreholes given by proposed discretization without regularization

N_{quad}^{heat}	64	128	256	512	1024
Condition number	294.8	352.6	69562	1.73×10^{11}	5.19×10^{18}
g(t=2a)	5.5324	5.5309	5.5282	5.5257	5.5248
g(t=4a)	6.1126	6.1107	6.1076	6.1049	6.1046
g(t=6a)	6.4385	6.4364	6.4331	6.4302	6.4315
g(t = 8a)	6.6607	6.6584	6.6550	6.6519	6.6593
g(t = 10a)	6.8267	6.8243	6.8207	6.8176	6.8360
g(t = 12a)	6.9576	6.9551	6.9515	6.9482	6.9944
g(t = 14a)	7.0647	7.0621	7.0584	7.0551	7.1801
g(t = 16a)	7.1546	7.1519	7.1481	7.1448	7.4290
g(t = 18a)	7.2315	7.2287	7.2249	7.2215	7.8758
g(t = 20a)	7.2983	7.2955	7.2917	7.2882	9.2351

Table 3: g-function of 2 boreholes given by uniform discretization without regularization

N_s	64	128	256	512	1024
Condition number	13.29	17.27	41.00	151.4	1116
g(t=2a)	5.5441	5.5409	5.5383	5.5361	5.5340
g(t=4a)	6.1259	6.1221	6.1192	6.1166	6.1143
g(t=6a)	6.4527	6.4486	6.4455	6.4428	6.4402
g(t = 8a)	6.6755	6.6712	6.6679	6.6651	6.6624
g(t = 10a)	6.8419	6.8375	6.8341	6.8311	6.8284
g(t = 12a)	6.9732	6.9686	6.9652	6.9622	6.9593
g(t = 14a)	7.0806	7.0759	7.0724	7.0693	7.0664
g(t = 16a)	7.1708	7.1660	7.1623	7.1592	7.1563
g(t = 18a)	7.2479	7.2430	7.2393	7.2362	7.2332
g(t = 20a)	7.3149	7.3100	7.3063	7.3031	7.3000

the converged value and even becomes negative. This unrealistic result is caused by the condition number of the linear system increasing quickly with the order of discretization that leads to numerical instability and incorrect results. The biggest condition number reaches 5.19×10^{18} and 2.27×10^{15} and renders the solutions to these ill-conditioned linear systems unreliable because thay are very sensitive to the perturbation and floating point error accumulated in the right hand side of 27 during computation. It contradicts the common intuition that more detailed discretization always provides more accurate value of g-function. Thus, the ill-conditioned problem we discussed in Section 2.4 is confirmed and the regularization method is necessary to improve the stability of solution.

3.1.2. Convergent g-functions with regularization

In the second round of test, we apply the regularization method to the linear system 27 with $\lambda = 1 \times 10^{-8}$ and solve the regularized linear system 41. The results are shown in Tables 6 to 9 and Figure 4.

We observe that the highest condition numbers of the linear system when the order of discretization equals to 1024 are reduced from 5.19×10^{18} to 1.48×10^{10} after regularization, which indicates that the regularization method improves the stability of the solution effectively. As shown in Figure 4, the values of g-function given by four methods all exhibit a clear trend to converge to a stable value as the order of discretization increases from 64 to 1024.

In terms of the convergence rate, it is obvious that the proposed discretization scheme converges faster than the other three methods including the optimal nonuniform discretization scheme in Figure 4. The proposed method reaches stable values of g-function at $N_{quad}^{heat}=512$ and more accurate than both uniform and nonuniform discretizations.

 $\hbox{ Table 4:} \ \underline{\textit{g-}} \hbox{function of 2 boreholes given by baseline nonuniform discretization without regularization} \\$

N_s	64	128	256	512	1024
Condition number	61.86	166.2	1811	175538	9.13×10^{8}
g(t=2a)	5.5369	5.5348	5.5327	5.5306	5.5285
g(t=4a)	6.1175	6.1151	6.1128	6.1104	6.1081
g(t=6a)	6.4437	6.4411	6.4386	6.4361	6.4336
g(t = 8a)	6.6661	6.6634	6.6607	6.6581	6.6555
g(t = 10a)	6.8322	6.8294	6.8267	6.8240	6.8212
g(t=12a)	6.9632	6.9603	6.9576	6.9548	6.9520
g(t = 14a)	7.0704	7.0675	7.0646	7.0618	7.0589
g(t = 16a)	7.1603	7.1574	7.1545	7.1516	7.1487
g(t = 18a)	7.2373	7.2343	7.2314	7.2284	7.2255
g(t = 20a)	7.3042	7.3011	7.2982	7.2952	7.2922

 $\begin{tabular}{ll} Table 5: g-function of 2 boreholes given by optimal nonuniform discretization without regularization \\ \end{tabular}$

N_s	64	128	256	512	1024
Condition number	765.6	16357	1.12×10^{7}	1.72×10^{13}	2.27×10^{15}
g(t=2a)	5.5331	5.5310	5.5290	5.5267	5.5258
g(t=4a)	6.1132	6.1109	6.1086	6.1060	6.1054
g(t=6a)	6.4391	6.4366	6.4341	6.4314	6.4347
g(t = 8a)	6.6612	6.6586	6.6560	6.6532	6.6380
g(t = 10a)	6.8272	6.8245	6.8218	6.8189	6.8487
g(t = 12a)	6.9581	6.9553	6.9526	6.9496	6.8483
g(t = 14a)	7.0652	7.0623	7.0595	7.0565	7.4772
g(t = 16a)	7.1550	7.1521	7.1493	7.1462	5.8117
g(t = 18a)	7.2319	7.2290	7.2261	7.2230	10.8160
g(t = 20a)	7.2987	7.2958	7.2928	7.2897	-3.5974

Table 6: g-function of 2 boreholes given by proposed discretization with regularization

N_{quad}^{heat}	64	128	256	512	1024
Condition number	294.8	352.6	69561	7.14×10^{9}	1.48×10^{10}
g(t=2a)	5.5324	5.5309	5.5282	5.5264	5.5263
g(t=4a)	6.1126	6.1107	6.1076	6.1057	6.1055
g(t=6a)	6.4385	6.4364	6.4331	6.4310	6.4308
g(t = 8a)	6.6607	6.6584	6.6550	6.6528	6.6526
g(t = 10a)	6.8267	6.8243	6.8207	6.8184	6.8182
g(t = 12a)	6.9576	6.9551	6.9515	6.9491	6.9489
g(t = 14a)	7.0647	7.0621	7.0584	7.0560	7.0558
g(t = 16a)	7.1546	7.1519	7.1481	7.1457	7.1455
g(t = 18a)	7.2315	7.2287	7.2249	7.2225	7.2222
g(t = 20a)	7.2983	7.2955	7.2917	7.2892	7.2889

Table 7: g-function of 2 boreholes given by uniform discretization with regularization

N_{quad}^{heat}	64	128	256	512	1024
Condition number	13.29	17.27	41.00	151.4	1116
g(t=2a)	5.5441	5.5409	5.5383	5.5361	5.5340
g(t=4a)	6.1259	6.1221	6.1192	6.1166	6.1143
g(t=6a)	6.4527	6.4486	6.4455	6.4428	6.4402
g(t = 8a)	6.6755	6.6712	6.6679	6.6651	6.6624
g(t=10a)	6.8419	6.8375	6.8341	6.8311	6.8284
g(t = 12a)	6.9732	6.9686	6.9652	6.9622	6.9593
g(t = 14a)	7.0806	7.0759	7.0724	7.0693	7.0664
g(t = 16a)	7.1708	7.1660	7.1623	7.1592	7.1563
g(t = 18a)	7.2479	7.2430	7.2393	7.2362	7.2332
g(t=20a)	7.3149	7.3100	7.3063	7.3031	7.3000

Table 8: g-function of 2 boreholes given by baseline nonuniform discretization with regularization

c. g ranction of 2 borono.	ico given oj	bubciliic i	onamorm	and conzum	on wrom regular
N_{quad}^{heat}	64	128	256	512	1024
Condition number	61.86	166.2	1811	175528	7.61×10^{8}
g(t=2a)	5.5369	5.5348	5.5327	5.5306	5.5286
g(t=4a)	6.1175	6.1151	6.1128	6.1104	6.1081
g(t=6a)	6.4437	6.4411	6.4386	6.4361	6.4336
g(t = 8a)	6.6661	6.6634	6.6607	6.6581	6.6555
g(t=10a)	6.8322	6.8294	6.8267	6.8240	6.8213
g(t=12a)	6.9632	6.9603	6.9576	6.9548	6.9520
g(t = 14a)	7.0704	7.0675	7.0646	7.0618	7.0590
g(t = 16a)	7.1603	7.1574	7.1545	7.1516	7.1487
g(t = 18a)	7.2373	7.2343	7.2314	7.2284	7.2255
g(t = 20a)	7.3042	7.3011	7.2982	7.2952	7.2923

Table 9: g-function of 2 boreholes given by optimal nonuniform discretization with regularization

one of granetien of 2 percentage given by optimize nondimenting discretization with regularization								
N_s	64	128	256	512	1024			
Condition number	765.6	16357	1.12×10^{7}	3.24×10^{9}	4.57×10^9			
g(t=2a)	5.5331	5.5310	5.5290	5.5276	5.5273			
g(t = 4a)	6.1132	6.1109	6.1086	6.1070	6.1067			
g(t=6a)	6.4391	6.4366	6.4341	6.4325	6.4321			
g(t = 8a)	6.6612	6.6586	6.6560	6.6543	6.6539			
g(t = 10a)	6.8272	6.8245	6.8218	6.8200	6.8196			
g(t = 12a)	6.9581	6.9553	6.9526	6.9507	6.9503			
g(t = 14a)	7.0652	7.0623	7.0595	7.0576	7.0572			
g(t = 16a)	7.1550	7.1521	7.1493	7.1474	7.1469			
g(t = 18a)	7.2319	7.2290	7.2261	7.2242	7.2237			
g(t = 20a)	7.2987	7.2958	7.2928	7.2909	7.2904			

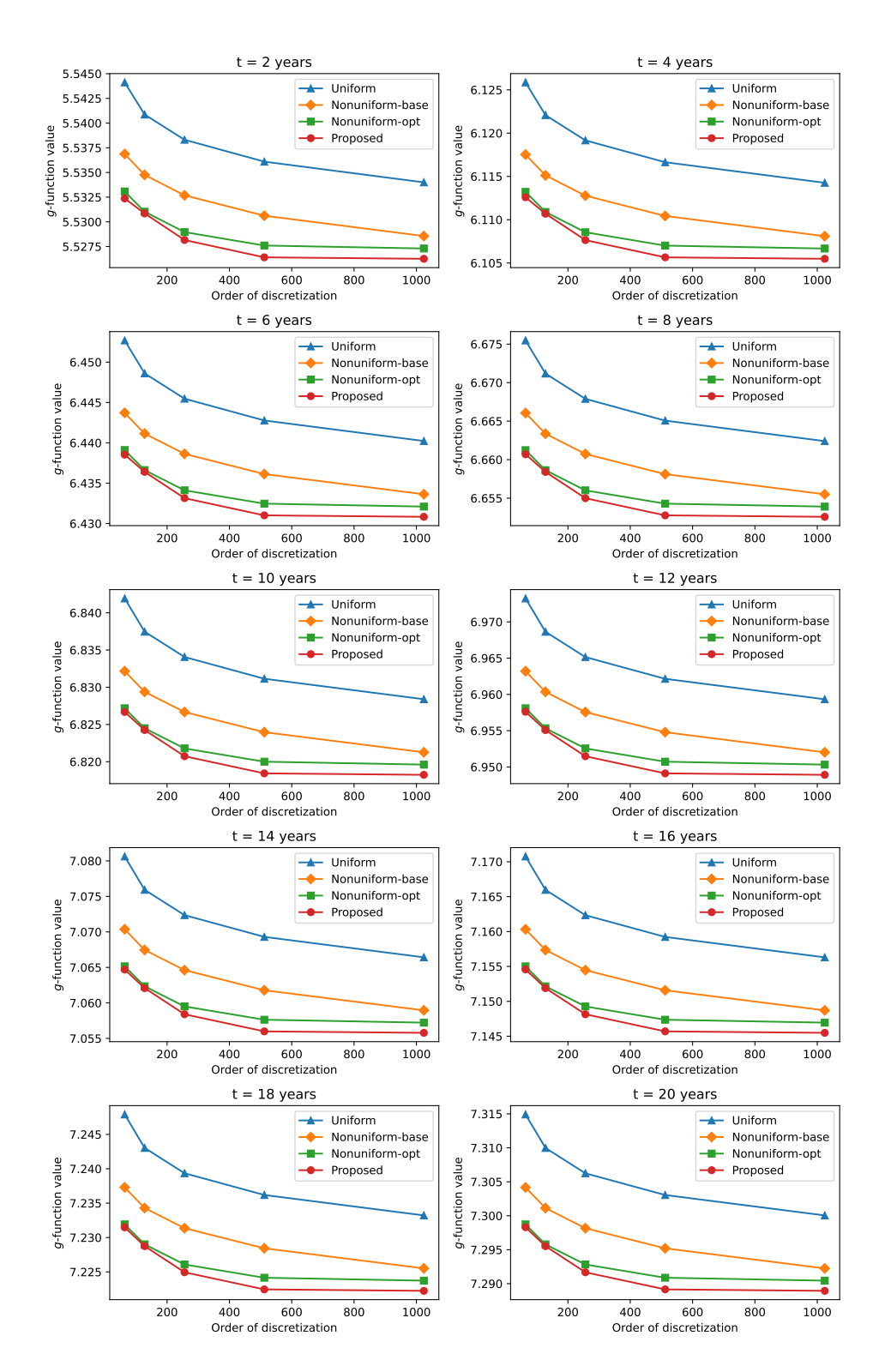


Figure 4: g-function of 2 boreholes given by different orders of discretization with regularization $\lambda = 1 \times 10^{-8}$

Table 10: Relative error of g-function given by the proposed discretization scheme with different combinations of N_{quad}^{heat} and N_{quad}^{temp} in 2 borehole test case

N_{quad}^{temp} N_{quad}^{temp}	64	128	256	512
2	-0.194141	-0.107730	-0.041976	-0.008899
3	0.339433	0.112407	0.024122	0.002487
5	0.165572	0.043313	0.005849	0.000239
10	-0.033025	-0.004897	0.000151	0.000028
25	0.003759	0.000929	0.000366	0.000029
50	0.001378	0.000881	0.000366	0.000029
75	0.001414	0.000881	0.000366	0.000029

3.2. Improvement on the computational efficiency and accuracy

The 2 borehole test case above has proved the necessity of regularization and the fast convergence rate of the proposed discretization to obtain accurate values of g-function compared with existing uniform and nonuniform discretization methods based on SFLS model. It also demonstrates the convergence behavior of g-function obtained by proposed discretization scheme as the number of quadrature points for heat N_{quad}^{heat} increases with fixed number of quadrature points for temperature in each interval $N_{quad}^{temp} = 40$. Now we further investigate how the proposed method improves the computational efficiency and accuracy of g-function compared with existing SFLS models.

Firstly, we analyze how the discretization to evaluate average temperature N_{quad}^{temp} influences the accuracy of g-function and how to select the appropriate combination of N_{quad}^{heat} and N_{quad}^{temp} to achieve the acceptable accuracy with the least computational cost.

We choose the same two boreholes as the test case and calculate the g-function at ten time points from 2 years to 20 years with the combination between $N_{quad}^{heat} = [64, 128, 256, 512]$ and $N_{quad}^{temp} = [2, 3, 5, 10, 25, 50, 75]$. The accuracy is evaluated by the relative error between the approximate value and the assumed exact value of g-function when $N_{quad}^{heat} = 1024$ and $N_{quad}^{temp} = 50$. The regularization parameter λ is set to 1×10^{-8} .

$$Error = \frac{\sum_{k=1}^{10} g_{approx}(t_k) - \sum_{k=1}^{10} g_{exact}(t_k)}{\sum_{k=1}^{10} g_{exact}(t_k)}$$
(42)

The results are shown in Table 10. We can observe that the relative error of g-function generally decreases as the number of quadrature points for heat N_{quad}^{heat} increases, which is consistent with the convergence rate we discussed before. When N_{quad}^{heat} is fixed, the relative error converges to a stable value with oscillations as the number of quadrature points to evaluate average temperature N_{quad}^{temp} in each interval increases. It is notable that the convergence rate with respect to N_{quad}^{temp} is much faster with bigger N_{quad}^{heat} . For example, the relative error of g-function with $N_{quad}^{heat} = 128$ converges to 0.000881 when $N_{quad}^{temp} = 50$, while the relative error with $N_{quad}^{heat} = 512$ converges to 0.000028 with only $N_{quad}^{temp} = 10$. This phenomenon is intuitive because when the interval to evaluate average temperature shrinks as N_{quad}^{heat} increases, its temperature distribution becomes more flat and we need fewer quadrature points N_{quad}^{temp} to approximate the average temperature in each interval.

The observation indicates that the value of N_{quad}^{temp} should be selected appropriately according to the order of discretization N_{quad}^{heat} . From the perspective of computational complexity, constructing the linear system 27 needs to compute the impact of $N_b N_{quad}^{heat}$ point heat sources on the temperature of $N_b N_{quad}^{heat} N_{quad}^{temp}$

Table 11: Configurations of discretization to compare the computational efficiency and accuracy

No	Proposed method $(N_{quad}^{heat}, N_{quad}^{temp})$	Other SFLS models (N_s)
1	(64, 50)	64
2	(128, 50)	128
3	(256, 25)	256
4	(512, 10)	512

Table 12: Comparison of the computational efficiency and accuracy in 2 borehole test case

No	No Proposed		Uniform		Nonuniform-base		Nonuniform-opt	
NO	Time(s)	Error	Time(s)	Error	Time(s)	Error	Time(s)	Error
1	0.09	1.4×10^{-3}	1.96	3.5×10^{-3}		2.0×10^{-3}		1.3×10^{-3}
2	0.41	$8.8 imes 10^{-4}$	10.71	2.8×10^{-3}	12.00	1.6×10^{-3}	10.70	9.2×10^{-4}
3	0.83	$3.7 imes10^{-4}$	46.89	2.3×10^{-3}	48.27	1.2×10^{-3}	52.54	5.2×10^{-4}
4	1.36	$2.8 imes10^{-5}$	190.1	1.9×10^{-3}	203.21	8.4×10^{-4}	222.78	2.6×10^{-4}

quadrature points, which has a $O(N_b^2 N_{quad}^{heat^2} N_{quad}^{temp})$ complexity proportional with N_{quad}^{temp} . Meanwhile, increasing N_{quad}^{temp} beyond the converging threshold indefinitely does not improve the accuracy of g-function significantly. Therefore, we suggest to set bigger N_{quad}^{temp} when N_{quad}^{heat} is small, and decrease N_{quad}^{temp} to a smaller value like 5 or 10 when N_{quad}^{heat} is sufficiently large to achieve a good balance between accuracy and computational cost.

Based on the analysis above, we choose the following 4 configurations of discretization to compare both the computational efficiency and accuracy of the proposed discretization scheme against existing methods in the 2 borehole test case as shown in Table 11.

The total computational time to evaluate the g-function from 2 years to 20 years and their relative errors given by four discretimization methods are shown in Table 12 with the following observations:

- 1. Three SFLS models with different discretization schemes exhibit similar computational efficiency with nearly quadratic complexity with respect to the order of discretization, because they all need to compare the $N_b^2N_s^2$ segment-to-segment response factors between N_bN_s segments. The computational time with 512 segments per borehole has exceeded 200 seconds even for the 2 borehole system. In contrast, the proposed discretization scheme is significantly faster with acceleration rate from 20 times to 160 times. The acceleration can be explained from two aspects: firstly the point-to-point heat response factor in our method is analytical and more efficient to compute than the segment-to-segment response factor containing double integral in SFLS models; secondly, the adaptive selection of discretization parameter (N_{quad}^{heat} , N_{quad}^{temp}) mitigates the $O(N_b^2N_{quad}^{heat^2}N_{quad}^{temp})$ complexity by reducing N_{quad}^{temp} for bigger N_{quad}^{heat} , thus the computational time grows slower than quadratic with respect to N_{quad}^{heat} and achieves higher acceleration rate under fine-grained discretization (160 times acceleration when $N_{quad}^{heat} = 512$ compared to 20 times acceleration when $N_{quad}^{heat} = 64$).
- 2. Besides the computational efficiency, the proposed discretization scheme also achieves better accuracy than existing methods especially in the context of fine-grained discretization (the only exception being the case with $N_{quad}^{heat}=64$ but the relative error is close to the optimal nonuniform discretization for SFLS model). The relative error of g-function given by the proposed method is less than 2.8×10^{-5} with $N_{quad}^{heat}=512$, while the relative error of SFLS models can only reach 2.6×10^{-4} even with the optimal nonuniform discretization. The proposed method achieves nearly 10 times improvement on accuracy compared to the best discretization scheme of SFLS models.

We also apply the proposed method to larger test cases with more boreholes including a 2x2 and 3x3 borehole configuration to demonstrate its accuracy and efficiency. We reduce the timespan to 10 years (5 timepoints from 2 years to 10 years) to decrease the computational cost and only compare the proposed

Table 13: Comparison of the computational efficiency and accuracy in 2×2 borehole test case

No	Proposed		Nonuniform-opt	
	Time(s)	Error	Time(s)	Error
1	0.21	1.5×10^{-3}	4.57	$1.4 imes 10^{-3}$
2	0.72	$9.1 imes 10^{-4}$	22.62	9.5×10^{-4}
3	1.56	$3.8 imes10^{-4}$	97.91	5.4×10^{-4}
4	2.67	$2.9 imes10^{-5}$	400.82	2.7×10^{-4}

Table 14: Comparison of the computational efficiency and accuracy in 3×3 borehole test case

No	Proposed		Nonuniform-opt	
	Time(s)	Error	Time(s)	Error
1	0.96	1.6×10^{-3}	22.63	$1.5 imes 10^{-3}$
2	3.84	$9.96 imes 10^{-4}$	106.43	1.03×10^{-3}
3	7.89	$4.1 imes 10^{-4}$	447.27	5.8×10^{-4}
4	14.3	$3.2 imes10^{-5}$	1874.84	2.9×10^{-4}

method with the optimal nonuniform discretization for SFLS model. The results are shown in Tables 13 and 14 and we can observe that the proposed method still achieves approximately 20-150 times better computational efficiency with close or better accuracy than the optimal nonuniform discretization for SFLS model.

4. Conclusions

This paper provides a novel discretization method for calculating g-functions of vertical geothermal boreholes, based on the direct numerical solution of the spatio-temporal integral equations that describe the thermal process. This method is significantly superior to the traditional SFLS model in both computational speed and accuracy, especially when using high-order discretization. Its core advantage lies in replacing the time-consuming segment-to-segment thermal response factors in the SFLS model, which require numerical integration, with point-to-point response factors that have an analytical form and are more efficient to compute. This methodological shift means that the g-function calculation no longer relies on empirical segmentation strategies but is instead theoretically supported by the Gauss-Legendre quadrature rule.

Furthermore, this paper identifies the g-function calculation problem as a Fredholm integral equation of the first kind and reveals the root cause for the divergence of calculation results at high discretization orders: the severe ill-conditioning of the discretized linear system. To solve this, we introduced a regularization technique that effectively overcomes this numerical instability, ensuring that the g-function values converge stably at any order of discretization.

The proposed method is valuable for applications such as optimization-based algorithms for borehole field design, which require a large number of simulations. Numerical tests clearly demonstrate its performance advantages: when processing a 3x3 borehole field, the proposed method reduces the computation time from 1874.84 seconds to just 14.3 seconds compared to the state-of-the-art nonuniform SFLS method, while simultaneously improving accuracy by nearly an order of magnitude.

References

- [1] I. Sarbu, C. Sebarchievici, General review of ground-source heat pump systems for heating and cooling of buildings, Energy and buildings 70 (2014) 441–454.
- [2] J. Luo, Q. Zhang, C. Liang, H. Wang, X. Ma, An overview of the recent development of the ground source heat pump (gshp) system in china, Renewable Energy 210 (2023) 269–279.
- [3] X. Wang, H. Zhang, L. Cui, J. Wang, C. Lee, X. Zhu, Y. Dong, Borehole thermal energy storage for building heating application: A review, Renewable and Sustainable Energy Reviews 203 (2024) 114772.
- [4] P. Eskilson, Thermal analysis of heat extraction boreholes (1987).

- [5] S. Rees, Advances in ground-source heat pump systems, Woodhead Publishing, 2016.
- [6] T. N. West, J. D. Spitler, Ground heat exchanger design tool with rowwise placement of boreholes, Science and Technology for the Built Environment 30 (9) (2024) 1148–1166.
- [7] X. Liu, J. D. Spitler, M. Qu, L. Shi, Recent developments in the design of vertical borehole ground heat exchangers for cost reduction and thermal energy storage, Journal of Energy Resources Technology 143 (10) (2021) 100803.
- [8] D. Marcotte, P. Pasquier, Fast fluid and ground temperature computation for geothermal ground-loop heat exchanger systems, Geothermics 37 (6) (2008) 651–665.
- [9] Y. Chen, B. Pan, X. Zhang, C. Du, Thermal response factors for fast parameterized design and long-term performance simulation of vertical gchp systems, Renewable energy 136 (2019) 793–804.
- [10] M. A. Bernier, P. Pinel, R. Labib, R. Paillot, A multiple load aggregation algorithm for annual hourly simulations of gchp systems, Hvac&R Research 10 (4) (2004) 471–487.
- [11] J. Claesson, S. Javed, A load-aggregation method to calculate extraction temperatures of borehole heat exchangers, ASHRAE transactions 118 (1) (2012) 530–540.
- [12] D. Pahud, G. Hellström, L. Mazzarella, Duct ground heat storage model for trnsys (trnvdst), Laboratory of Energy Systems, Lausanne (1997).
- [13] Y. L. E. Law, S. B. Dworkin, Characterization of the effects of borehole configuration and interference with long term ground temperature modelling of ground source heat pumps, Applied Energy 179 (2016) 1032–1047.
- [14] X. Yang, W. Cai, Y. Li, M. Wang, Y. Kong, F. Wang, C. Chen, Numerical investigation on the influence of groundwater flow on long-term heat extraction performance of deep borehole heat exchanger array, Geothermal Energy 12 (1) (2024) 45
- [15] H. Y. Zeng, N. R. Diao, Z. H. Fang, A finite line-source model for boreholes in geothermal heat exchangers, Heat Transfer Asian Research 31 (7) (2002) 558–567.
- [16] L. Lamarche, B. Beauchamp, A new contribution to the finite line-source model for geothermal boreholes, Energy and buildings 39 (2) (2007) 188–198.
- [17] P. Cui, H. Yang, Z. Fang, Heat transfer analysis of ground heat exchangers with inclined boreholes, Applied thermal engineering 26 (11-12) (2006) 1169–1175.
- [18] D. Marcotte, P. Pasquier, The effect of borehole inclination on fluid and ground temperature for glhe systems, Geothermics 38 (4) (2009) 392–398.
- [19] L. Lamarche, A fast algorithm for the hourly simulations of ground-source heat pumps using arbitrary response factors, Renewable Energy 34 (10) (2009) 2252–2258.
- [20] M. Fossa, The temperature penalty approach to the design of borehole heat exchangers for heat pump applications, Energy and Buildings 43 (6) (2011) 1473–1479.
- [21] M. Cimmino, M. Bernier, A semi-analytical method to generate g-functions for geothermal bore fields, International Journal of Heat and Mass Transfer 70 (2014) 641–650.
- [22] P. Monzo, P. Mogensen, J. Acuña, F. Ruiz-Calvo, C. Montagud, A novel numerical approach for imposing a temperature boundary condition at the borehole wall in borehole fields, Geothermics 56 (2015) 35–44.
- [23] A. Lazzarotto, A methodology for the calculation of response functions for geothermal fields with arbitrarily oriented boreholes—part 1, Renewable Energy 86 (2016) 1380–1393.
- [24] A. Lazzarotto, F. Björk, A methodology for the calculation of response functions for geothermal fields with arbitrarily oriented boreholes—part 2, Renewable energy 86 (2016) 1353—1361.
- [25] M. Cimmino, The effects of borehole thermal resistances and fluid flow rate on the g-functions of geothermal bore fields, International Journal of Heat and Mass Transfer 91 (2015) 1119–1127.
- [26] M. Cimmino, Semi-analytical method for g-function calculation of bore fields with series-and parallel-connected boreholes, Science and Technology for the Built Environment 25 (8) (2019) 1007–1022.
- [27] M. Cimmino, g-functions for fields of series-and parallel-connected boreholes with variable fluid mass flow rate and reversible flow direction, Renewable Energy 228 (2024) 120661.
- [28] M. Cimmino, D. Thorne, C. Langevin, M. Sukop, Pygfunction: an open-source toolbox for the evaluation of thermal response factors for geothermal borehole fields, Proceedings of eSim 2018 (2018).
- [29] M. Cimmino, J. C. Cook, pygfunction 2.2: New features and improvements in accuracy and computational efficiency (2022).
- [30] J. C. Cook, Development of computer programs for fast computation of g-functions and automated ground heat exchanger design, Master's thesis, Oklahoma State University (2021).
- [31] L. Lamarche, G-function generation using a piecewise-linear profile applied to ground heat exchangers, International Journal of Heat and Mass Transfer 115 (2017) 354–360.
- [32] M. Cimmino, J. C. Cook, J. A. Isiordia Farrera, Optimal discretization of geothermal boreholes for the calculation of g-functions, Science and Technology for the Built Environment 30 (3) (2024) 234–249.
- [33] H. S. Carslaw, J. C. Jaeger, Conduction of Heat in Solids, 2nd Edition, Oxford University Press, Oxford, 1986.
- [34] J. Claesson, S. Javed, An analytical method to calculate borehole fluid temperatures for time-scales from minutes to decades., ASHRAE Transactions 117 (2) (2011).
- [35] W. Hackbusch, Integral equations: theory and numerical treatment, Vol. 120, Birkhäuser, 2012.
- [36] A.-M. Wazwaz, Linear and nonlinear integral equations, Vol. 639, Springer, 2011.
- [37] A.-M. Wazwaz, The regularization method for fredholm integral equations of the first kind, Computers & Mathematics with Applications 61 (10) (2011) 2981–2986.